

Abnormal Seebeck effect in doped conducting polymers

Cite as: Appl. Phys. Lett. **118**, 123301 (2021); <https://doi.org/10.1063/5.0043863>

Submitted: 11 January 2021 . Accepted: 11 March 2021 . Published Online: 22 March 2021

 Yufei Ge,  Ran Liu, and  Zhigang Shuai

COLLECTIONS

Paper published as part of the special topic on [Organic and Hybrid Thermoelectrics](#)



View Online



Export Citation



CrossMark

ARTICLES YOU MAY BE INTERESTED IN

[Differential charge boost in hysteretic ferroelectric–dielectric heterostructure capacitors at steady state](#)

Applied Physics Letters **118**, 122901 (2021); <https://doi.org/10.1063/5.0035880>

[Optoelectronic superlattices based on 2D transition metal dichalcogenides](#)

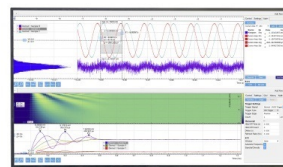
Applied Physics Letters **118**, 123101 (2021); <https://doi.org/10.1063/5.0044509>

[Loss channels affecting lithium niobate phononic crystal resonators at cryogenic temperature](#)

Applied Physics Letters **118**, 123501 (2021); <https://doi.org/10.1063/5.0034909>

Challenge us.

What are your needs for periodic signal detection?



Zurich Instruments



Abnormal Seebeck effect in doped conducting polymers

Cite as: Appl. Phys. Lett. **118**, 123301 (2021); doi: [10.1063/5.0043863](https://doi.org/10.1063/5.0043863)

Submitted: 11 January 2021 · Accepted: 11 March 2021 ·

Published Online: 22 March 2021



View Online



Export Citation



CrossMark

Yufei Ge, Ran Liu, and Zhigang Shuai^{a)}

AFFILIATIONS

MOE Key Laboratory of Organic OptoElectronics and Molecular Engineering, Department of Chemistry, Tsinghua University, 100084 Beijing, People's Republic of China

Note: This paper is part of the APL Special Collection on Organic and Hybrid Thermoelectrics.

^{a)} Author to whom correspondence should be addressed: zgshuai@tsinghua.edu.cn

ABSTRACT

The Seebeck effect or thermopower relates the temperature gradient to the electric voltage drop. Seebeck coefficient α measures the transport entropy, which could either linearly increase with temperature T like metallic conducting or decrease as $1/T$ like semiconducting behavior. It could become more complicated in the temperature dependence for a number of disordered systems but still in a monotonic way. However, several recent experiments reported the “abnormal” non-monotonic temperature dependence of the Seebeck coefficient in doped conducting polymers, for instance, first increasing and then decreasing. Through a one-dimensional tight-binding model coupled with the Boltzmann transport equation, we investigate theoretically the doping effect for the Seebeck coefficient. We find that the abnormal behavior comes from multi bands' contribution and a two-band model (conduction or valence band plus a narrow polaronic band) can address such an abnormal Seebeck effect, namely, if there exists (i) a small bandgap accessible for thermal activation between the two bands; and (ii) a large difference in the bandwidth between the polaronic band and the conduction band (or valence band), then the Seebeck coefficient increases with temperature first, then levels off, and finally drops down.

Published under license by AIP Publishing. <https://doi.org/10.1063/5.0043863>

Conducting polymers for thermoelectric applications have attracted growing research interest in the past few decades with the figure of merit ZT increasing from 10^{-3} to 0.4.^{1–5} Seebeck coefficient α measures the voltage drop with respect to the temperature gradient and is regarded as “transport entropy,”⁶ namely, the occupation entropy changes with respect to carrier numbers. There have been a number of models proposed earlier in the literature for the thermoelectric transport behavior in conducting polymers, ranging from metallic^{7,8} to semiconducting⁹ behavior and to several hopping mechanisms such as mobility edge,¹⁰ variable range hopping,^{11,12} and Efros–Shklovskii hopping.¹³ Even though these differ enormously over the transport mechanisms,¹⁴ these all demonstrated the monotonic temperature dependence, decreasing or increasing. Nevertheless, non-monotonic temperature dependences of the Seebeck coefficient have been observed in conducting polymer systems for which the absolute value of the Seebeck coefficient increases quickly at low temperature but decreases at high temperature.^{5,15–17} Previously, it has been considered to combine two models, one for the increase and the other for the decrease with temperature.¹⁸ However, it lacks a unified physical rationalization. By performing density functional theory computation

coupled with the Boltzmann transport equation considering phonon scattering and impurity scattering terms, we have demonstrated that the doping-induced polaronic band can boost the thermoelectric power factor in potassium-doped metal-coordinated polymers, and at a low doping concentration, the Seebeck coefficient increases with temperature, then levels off, and finally decreases with temperature.¹⁹ In this work, we term such atypical temperature behavior as the “abnormal Seebeck effect,” and we will illustrate such atypical temperature behavior from a tight-binding study.

We take an n -type doped conducting polymer as an example, which is modeled by the following Hamiltonian:

$$\hat{H} = \sum_i \varepsilon \hat{a}_i^\dagger \hat{a}_i + \sum_i \beta \left(\hat{a}_i^\dagger \hat{a}_{i+1} + \hat{a}_{i+1}^\dagger \hat{a}_i \right). \quad (1)$$

As shown in Fig. 1(a), site index i represents the lowest unoccupied molecular orbital (LUMO) for i th unit cell with energy ε and only nearest-neighbor hopping integral β is taken into account. For n -type doping, dopant orbital's interaction with the main chain is also included in site energy difference $\Delta\varepsilon$ and hopping integral β' . For N unit cells, there is one dopant. The periodic boundary condition is

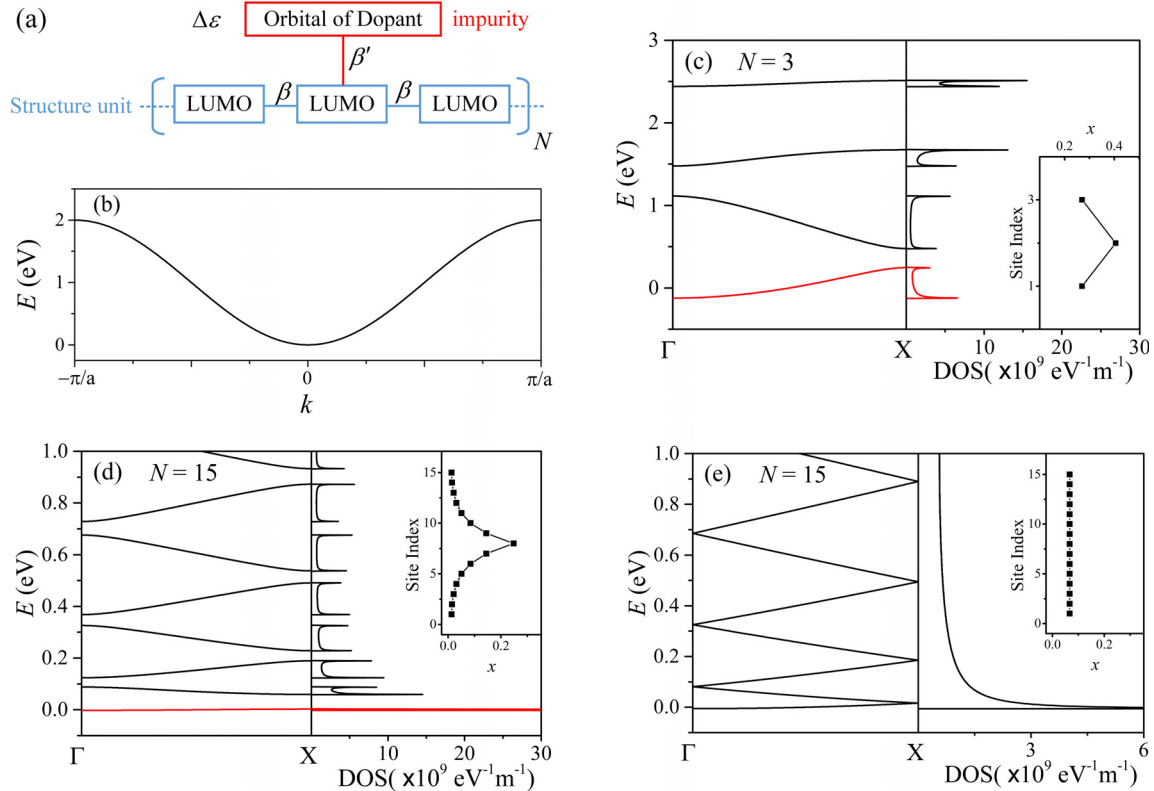


FIG. 1. (a) Graphic illustration of the tight-binding model employed in our work. (b) Band structure of the undoped chain with $\beta = -0.5$ eV and $\varepsilon = 1.0$ eV. The calculated band structures and density of states (DOS) with $1 : N$ doping are plotted in (c) and (d). Here, we set $\beta = -0.5$ eV, $\Delta\varepsilon = 1.0$ eV, $\beta' = 1.5\beta$, and $E_F = 0$. We observe the formation of a half-filling doping-induced polaronic band (red) whose charge distribution x is plotted as well. We also plot calculated band structures, density of states (DOS), and charge distribution in (e) when $\beta = -0.5$ eV, $\Delta\varepsilon = 1.0$ eV, and $\beta' = 0$. Note that charge is totally delocalized in the whole chain when $\beta' = 0$.

adopted to calculate the band structure. The length of a structure unit a is set as 20 a.u. (*ca.* 1.06 nm) for simplicity, and the size of a unit cell is Na .

The Boltzmann transport equation^{20,21} was employed to calculate conductivity σ and Seebeck coefficient α . The conductivity $\sigma = \sum_j \sigma_j$ is the summation over all bands and Seebeck coefficient $\alpha = \frac{1}{\sigma} \sum_j \alpha_j \sigma_j$ is weighted average of each band's Seebeck coefficient based on conductivity. In our one-dimensional model,

$$\sigma_j = e^2 \sum_k \left(-\frac{\partial f}{\partial E} \right) v_k v_k \tau_k, \quad (2)$$

$$\alpha_j = \frac{e}{\sigma_j} \sum_k \frac{E - E_F}{T} \left(-\frac{\partial f}{\partial E} \right) v_k v_k \tau_k, \quad (3)$$

where $v_k = \frac{1}{\hbar} \frac{\partial E}{\partial k}$ is the group velocity, j is the label of the bands, and $f = 1 / \{1 + \exp[(E - E_F) / k_B T]\}$ is the Fermi distribution function.

According to Matthiessen's rule,¹⁹ the relaxation time τ is expressed as

$$\tau^{-1} = \tau_{ph}^{-1} + \tau_{imp}^{-1}, \quad (4)$$

where τ_{ph} is the relaxation time related to electron-phonon scattering. According to deformation potential theory,²⁰

$$\frac{1}{\tau_{ph}} = \frac{2\pi k_B T E_1^2}{\hbar C_{ii}} \sum_k \delta(E_k - E_k') (1 - \cos \theta), \quad (5)$$

where C_{ii} , E_1 , and θ are the elastic constant, deformation potential constant, and scattering angle, respectively. Considering (i) scattering angle θ is either 0 or π in a one-dimensional system and (ii) the calculated band structures shown in Fig. 1 are monotonic in $[0, \pi/Na]$, we can approximate Eq. (5) as $\tau_{ph}^{-1} = A_1 T$, where A_1 is a wave vector independent constant.

τ_{imp} is the relaxation time related to electron-impurity scattering. As a primitive approximation,²² we postulate $\tau_{imp}^{-1} = A_2 / (N + 1)$, which is proportional to the concentration of impurities and independent of temperature. Thus, the following relaxation time formula is obtained:

$$\tau = [A_1 T + A_2 / (N + 1)]^{-1}. \quad (6)$$

Here, A_1 and A_2 are constants to be fitted by first-principles calculations. From Ref. 23, we obtain $A_1 = 10^{10} \text{ s}^{-1} \text{ K}^{-1}$ and $A_2 = 10^{13} \text{ s}^{-1}$.

As shown in Fig. 1(b), the conduction band of the undoped chain is formed by the interaction between the lowest unoccupied molecular orbitals (LUMOs) for the unit cell. The band structures and density of states (DOS) after doping are presented in Figs. 1(c) and 1(d). Here, we set $\beta = -0.5$ eV and $\Delta\varepsilon = 1.0$ eV by fitting previous

first-principles calculations.^{19,21} $\beta' = 1.5\beta$ was set to make the doping effect more pronounced. When β' is nonzero, the original translational symmetry is broken, so a series of separate bands are formed. Namely, with $1 : N$ doping, the wide and continuous band of the pristine polymer splits into N separated bands. The bottom band is half-filling, and it is quite narrow when N is large.

Charge distribution is calculated through orbitals' combination coefficient and is also included in Figs. 1(c) and 1(d). About 95% charge transfer from the dopant to the chain when $\beta' = 1.5\beta$. When lightly doped, according to the calculated charge distribution of the narrow half-filling band in Fig. 1(d), charge mainly localizes at the units close to the dopant and the charge density decreases quickly away from dopant site. Combined with Fig. 1(e), the localization of the charge carrier in the narrow band results from the additional interaction between the LUMO of the structure unit and orbital of dopants, which stabilizes electrons near the dopant. These localized states are generally accompanied by lattice distortion, which stabilizes localized states further.²⁴ Considering the bottom band is narrow, half-filling, and formed by doping-induced localized states, we term this band as the "doping induced polaronic band (PB)."²⁵ As shown in Fig. 1(d), bands above the PB are relatively much wider, preserving the delocalized nature of pristine conducting polymer's conduction band. In addition, the bandgap between the PB and the conduction band (CB) is small that the thermal activation can be expected to play an essential role in transport phenomena.

For a specific doped conducting polymer system, β , β' , and $\Delta\varepsilon$ are constant at different doping levels. Several features of band structures at different doping levels can be notified, as shown in Fig. 2. Namely, both the bandwidth of doping-induced polaronic band W_{PB} and the bandgap Δ between the PB and the CB decrease with N .

Temperature dependences of conductivity and the Seebeck coefficient at different doping levels are calculated through Boltzmann transport theory in Fig. 3. When heavily doped ($N = 3$), conductivity decreases with increasing temperature and the Seebeck coefficient increases linearly with increasing temperature, revealing a metallic transport behavior.⁹ However, an abnormal nonmonotonic temperature dependence is observed in lightly doped systems ($N = 21$). As temperature increases, conductivity decreases in the low temperature region, indicating a metallic behavior. However, as temperature keeps increasing, the conductivity will increase dramatically with increasing

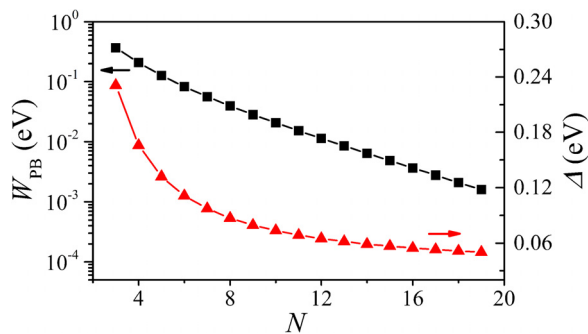


FIG. 2. Dependence of the bandwidth of PB W_{PB} and the bandgap between the PB and CB Δ . Here, $\beta = -0.5$ eV, $\Delta\varepsilon = 1.0$ eV, and $\beta' = 1.5\beta$.

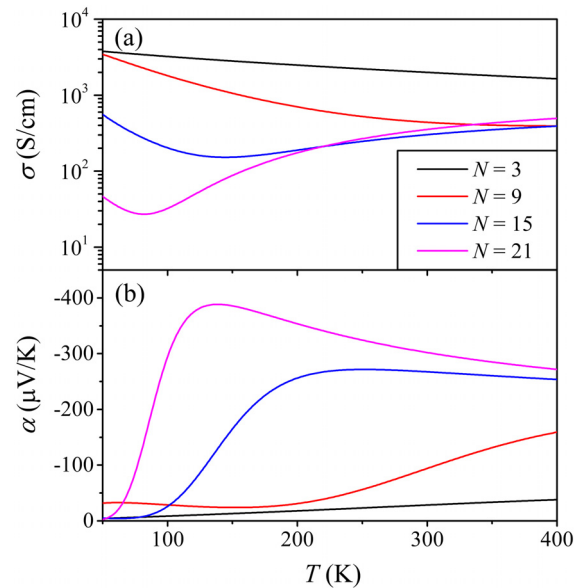


FIG. 3. Temperature dependence of (a) conductivity and (b) the Seebeck coefficient at different doping levels. An abnormal Seebeck effect is observed when lightly doped.

temperature, which reveals a thermally activated transport behavior. This nonmonotonic temperature dependence was reported in experiments.^{5,26} Meanwhile, in the low temperature region, a boost of the Seebeck coefficient with increasing temperature is observed. After the arrival of maximum, the Seebeck coefficient levels off and finally decreases with increasing temperature. This temperature dependence agrees with phenomena observed in experiments^{5,15–17} and is termed as the abnormal Seebeck effect in our work.

To understand this abnormal Seebeck effect, we calculate the temperature dependence of conductivity and the Seebeck coefficient with different numbers of the band. In Figs. 4(a) and 4(b), the conductivity and Seebeck coefficient are mainly contributed by the PB in the full temperature region when heavily doped ($N = 3$). In Figs. 4(c) and 4(d), a multi-band transport behavior is observed when lightly doped ($N = 21$). If we only consider PB's contribution, transport behavior significantly differs from the total behavior. A critical change is observed when we consider the bottom two bands, i.e., the PB and CB. In this case, the conductivity decreases with increasing temperature in the low temperature region and increases in the high temperature region, while the Seebeck coefficient increases first and finally decreases. When more bands are considered, the transport behavior keeps approaching the total behavior and coincides if bottom 6 bands are considered. In summary, the abnormal Seebeck effect is a multi-band effect and a similar tendency can be observed when bottom two bands are considered. The graphical illustration is presented in Fig. 5.

To elucidate the different temperature dependence at different doping levels, a simplified two-band model is considered here to explain Figs. 4(c) and 4(d). Namely, only the half-filling PB and CB shown in Fig. 5 are considered to analyze the different temperature

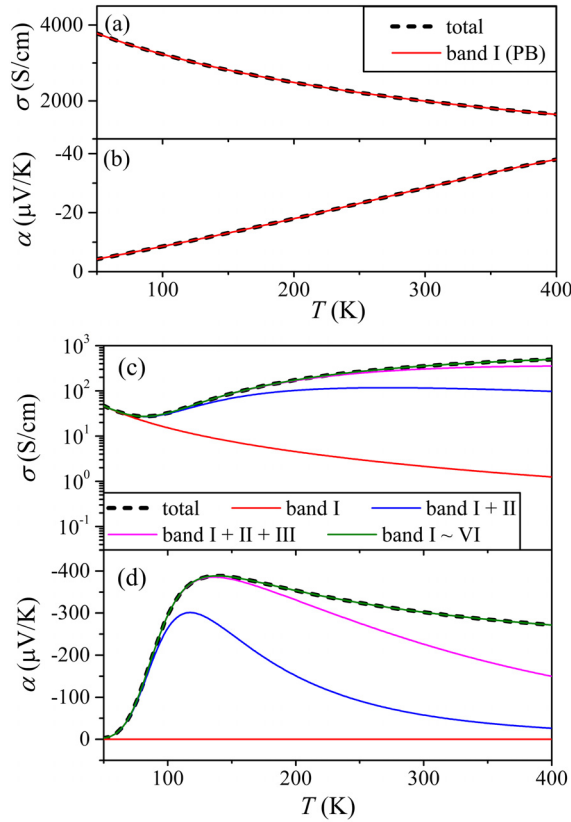


FIG. 4. Calculated temperature dependence of conductivity and the Seebeck coefficient with different numbers of bands considered when $N = 3$ (a) and (b) and $N = 21$ (c) and (d). Bands are labeled from bottom to top by roman numerals: I (i.e., PB), II (i.e., CB), III, IV, V, etc.

dependence. In the two-band model, the total conductivity and Seebeck coefficient can be expressed as follows:

$$\begin{cases} \sigma = \sigma_{PB} + \sigma_{CB} \\ \alpha = \frac{\alpha_{PB}\sigma_{PB} + \alpha_{CB}\sigma_{CB}}{\sigma_{PB} + \sigma_{CB}} \end{cases} \quad (7)$$

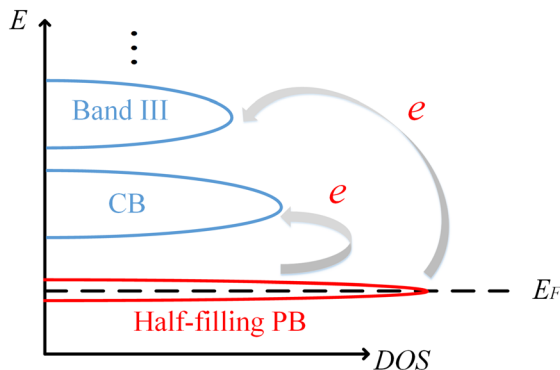


FIG. 5. Abstract band structure when lightly doped. Bands close to the Fermi level contribute to conductivity and the Seebeck coefficient.

Obviously, the band with the larger conductivity will dominate the thermoelectric behavior. A ratio σ_{CB}/σ_{PB} is defined to measure the relative conductivity:

$$\frac{\sigma_{CB}}{\sigma_{PB}} = \frac{e^2 \sum_{k,CB} (-\partial f / \partial E) v_k v_k \tau_k}{e^2 \sum_{k,PB} (-\partial f / \partial E) v_k v_k \tau_k} \quad (8)$$

Considering the periodicity and symmetry of band structures, we postulate

$$E(k) = W \sum_{n=1}^{\infty} b_n \cos nNak + constant, \quad (9)$$

where W is the bandwidth and b_n is constant depending on the shape of energy bands. Thus,

$$\sum_k v_k v_k = W^2 \int_{-\pi/Na}^{\pi/Na} \left[\sum_{n=1}^{\infty} \frac{nNab_n}{\hbar} \sin nNak \right]^2 dk = BW^2. \quad (10)$$

Here, B is a constant calculated from the integral.

For Fermi distribution,

$$-\frac{\partial f}{\partial E} = \frac{f(1-f)}{k_B T}, \quad f = \left[1 + \exp\left(\frac{E - E_F}{k_B T}\right) \right]^{-1}. \quad (11)$$

When $E - E_F$ is small, as is the case in the PB, we make approximation $E - E_F = 0$ and substitute to Eq. (11). Then,

$$-\frac{\partial f}{\partial E} = \frac{1}{4k_B T}. \quad (12)$$

When $E - E_F$ is relatively large, as is the case in the CB, $f \ll 1$,

$$-\frac{\partial f}{\partial E} \approx \frac{f}{k_B T} \approx \frac{1}{k_B T [1 + \exp(\Delta/k_B T)]}. \quad (13)$$

Here, considering that the PB is very narrow, we make approximation $E - E_F \approx \Delta$ in Eq. (13) further, where Δ is the bandgap.

Substituting Eqs. (6), (10), (12), and (13) into Eq. (8), we get

$$\frac{\sigma_{CB}}{\sigma_{PB}} = Constant \times \left(\frac{W_{CB}}{W_{PB}} \right)^2 \frac{1}{[1 + \exp(\Delta/k_B T)]}. \quad (14)$$

Equation (14) reveals that a small bandgap plus a large CB bandwidth leads the CB to play a dominant important role in finite temperature transport.

Therefore, we shall discuss the following two cases:

- (i) When heavily doped, i.e., N is small. As shown in Fig. 2, the PB is wide and the bandgap between the PB and the CB is relatively large. Consequently, the PB dominates transport, which leads to a metallic band-like transport behavior.
- (ii) When lightly doped, i.e., N is large. The narrow PB indicates a large ratio W_{CB}/W_{PB} and the small bandgap Δ enhances thermal activation. These make the CB dominate the conductivity and Seebeck coefficient as thermal activation for high temperature. However, the PB still dominates the conductivity in the low temperature region. Therefore, a metallic-like decrease in conductivity with increasing

temperature is observed in the low temperature region. While in the high temperature region, conductivity increases with increasing temperature because of increasing thermal activation.

Different from the wide PB in *case (i)*, the PB in *case (ii)* is narrow. In a narrow band limit, the Seebeck coefficient of a half-filling band is so small that can be ignored.⁶ Therefore, a further approximation is reliable:

$$\alpha = \frac{\alpha_{PB}\sigma_{PB} + \alpha_{CB}\sigma_{CB}}{\sigma_{PB} + \sigma_{CB}} \approx \frac{\alpha_{CB}\sigma_{CB}}{\sigma_{PB} + \sigma_{CB}} = \frac{\alpha_{CB}}{\sigma_{PB}/\sigma_{CB} + 1}, \quad (15)$$

where⁹

$$\alpha_{CB} = \frac{A_3}{T} + A_4. \quad (16)$$

Here, A_3 and A_4 are temperature independent constants.

In the low temperature region, the PB dominates the conductivity and the total Seebeck coefficient is

$$\alpha_{LT} = \frac{\alpha_{CB}}{\sigma_{PB}/\sigma_{CB} + 1} \approx \alpha_{CB} \frac{\sigma_{CB}}{\sigma_{PB}}. \quad (17)$$

Substituting Eqs. (14) and (16) into Eq. (17) and calculating the derivative, we will find that the Seebeck coefficient increases with increasing temperature as a result of thermal activation.

In the high temperature region, the CB dominates the conductivity and the PB has no influence on transport behavior other than pinning the Fermi level inside itself. Consequently, we obtain a semiconductor-like temperature dependence of the total Seebeck coefficient:

$$\alpha_{HT} = \frac{\alpha_{CB}}{\sigma_{PB}/\sigma_{CB} + 1} \approx \alpha_{CB} \approx \frac{A_3}{T} + A_4. \quad (18)$$

Thus, the Seebeck coefficient decreases with increasing temperature in the high temperature region.

In summary, we employ a tight-binding model to analyze the abnormal Seebeck effect observed in recent experiments. The doping-induced narrow and half-filled polaronic band plays an essential role. Through the Boltzmann transport equation, for the light doping case, the Seebeck coefficient increases first, then levels off, and finally decreases. A simple two-band model (a narrow polaronic band plus a wide conduction band) is adopted. For the lightly doped polymer, we find that (i) a small bandgap is accessible for thermal activation between two bands and (ii) there exists a large difference in the bandwidth between the two bands. Then, at low temperature, the polaronic band dominates transport, leading to a decrease in conductivity but an increase in the Seebeck coefficient with temperature. Then, at higher temperature, the conduction band participates in transport through thermal activation, leading to an increase in conductivity and a decrease in the Seebeck coefficient. However, for the heavily doped polymer, since the polaronic band is quite wide and the gap to the CB is large, only normal metallic behavior can be observed. We note that during the recent rush for high ZT nanomaterials, similar abnormal

Seebeck effects have also been found in Sb-doped PbSe or SnSe and its potassium/sodium/lithium doped polycrystals.^{27,28}

This work was supported by the National Natural Science Foundation of China (Grant No. 21788102) and the Ministry of Science and Technology of the People's Republic of China (Grant No. 2017YFA0204501).

DATA AVAILABILITY

The data that support the findings of this study are available from the corresponding author upon reasonable request.

REFERENCES

- ¹F. X. Jiang, J. K. Xu, B. Y. Lu, Y. Xie, R. J. Huang, and L. F. Li, *Chin. Phys. Lett.* **25**, 2202 (2008).
- ²O. Bubnova, Z. U. Khan, A. Malti, S. Braun, M. Fahlman, M. Berggren, and X. Crispin, *Nat. Mater.* **10**, 429 (2011).
- ³G. H. Kim, L. Shao, K. Zhang, and K. P. Pipe, *Nat. Mater.* **12**, 719 (2013).
- ⁴C. Wan, X. Gu, F. Dang, T. Itoh, Y. Wang, H. Sasaki, M. Kondo, K. Koga, K. Yabuki, G. J. Snyder, R. Yang, and K. Koumoto, *Nat. Mater.* **14**, 622 (2015).
- ⁵Y. Sun, L. Qiu, L. Tang, H. Geng, H. Wang, F. Zhang, D. Huang, W. Xu, P. Yue, Y. S. Guan, F. Jiao, Y. Sun, D. Tang, C. A. Di, Y. Yi, and D. Zhu, *Adv. Mater.* **28**, 3351 (2016).
- ⁶D. M. Rowe, *Thermoelectrics Handbook: Macro to Nano* (CRC Press, Boca Raton, 2006).
- ⁷M. Cutler and N. F. Mott, *Phys. Rev.* **181**, 1336 (1969).
- ⁸S. Watanabe, M. Ohno, Y. Yamashita, T. Terashige, H. Okamoto, and J. Takeya, *Phys. Rev. B* **100**, 241201(R) (2019).
- ⁹H. Fritzsche, *Solid State Commun.* **9**, 1813 (1971).
- ¹⁰N. F. Mott and E. A. Davis, *Electronic Processes in Non-Crystalline Materials*, 2nd ed. (Oxford University Press, Oxford, 2012).
- ¹¹R. Schmechel, *J. Appl. Phys.* **93**, 4653 (2003).
- ¹²N. Tessler, Y. Preezant, N. Rappaport, and Y. Roichman, *Adv. Mater.* **21**, 2741 (2009).
- ¹³A. L. Efros and B. I. Shklovskii, *J. Phys. C* **8**, L49 (1975).
- ¹⁴K. Asadi, A. J. Kronemeijer, T. Cramer, L. J. Koster, P. W. Blom, and D. M. de Leeuw, *Nat. Commun.* **4**, 1710 (2013).
- ¹⁵C.-G. Wu, D. C. DeGroot, H. O. Marcy, J. L. Schindler, C. R. Kannewurf, Y.-J. Liu, W. Hirpo, and M. G. Kanatzidis, *Chem. Mater.* **8**, 1992 (1996).
- ¹⁶N. Tushima, M. Imai, and S. Ichikawa, *J. Electron. Mater.* **40**, 898 (2011).
- ¹⁷S. R. S. Kumar, N. Kurra, and H. N. Alshareef, *J. Mater. Chem. C* **4**, 215 (2016).
- ¹⁸B. Sixou, N. Mermilliod, and J. P. Travers, *Phys. Rev. B* **53**, 4509 (1996).
- ¹⁹Y. Liu, W. Shi, T. Zhao, D. Wang, and Z. Shuai, *J. Phys. Chem. Lett.* **10**, 2493 (2019).
- ²⁰D. Wang, W. Shi, J. Chen, J. Xi, and Z. Shuai, *Phys. Chem. Chem. Phys.* **14**, 16505 (2012).
- ²¹W. Shi, T. Zhao, J. Xi, D. Wang, and Z. Shuai, *J. Am. Chem. Soc.* **137**, 12929 (2015).
- ²²N. W. Ashcroft and N. D. Mermin, *Solid State Physics* (Harcourt, Orlando, 1976).
- ²³W. Shi, D. Wang, and Z. Shuai, *Adv. Electron. Mater.* **5**, 1800882 (2019).
- ²⁴D. Emin, *Polarons* (Cambridge University Press, Cambridge, 2013).
- ²⁵S. Stafstrom and J. L. Bredas, *Phys. Rev. B* **38**, 4180 (1988).
- ²⁶N. Massonnet, A. Carella, A. de Geyer, J. Faure-Vincent, and J. P. Simonato, *Chem. Sci.* **6**, 412 (2015).
- ²⁷L. D. Zhao, S. H. Lo, Y. S. Zhang, H. Sun, G. J. Tan, C. Uher, C. Wolverton, V. P. Dravid, and M. G. Kanatzidis, *Nature* **508**, 373 (2014).
- ²⁸T. R. Wei, G. J. Tan, X. M. Zhang, C. F. Wu, J. F. Li, V. P. Dravid, G. J. Snyder, and M. G. Kanatzidis, *J. Am. Chem. Soc.* **138**, 8875 (2016).